LETTERS
PUBLISHED ONLINE: 20 DECEMBER 2009 | DOI: 10.1038/NPHYS1483
nature physics

Normal-state spin dynamics and temperature-dependent spin-resonance energy in optimally doped $BaFe_{1.85}Co_{0.15}As_2$

D. S. Inosov[1], J. T. Park[1], P. Bourges[2], D. L. Sun[1], Y. Sidis[2], A. Schneidewind[3,4], K. Hradil[4,5], D. Haug[1], C. T. Lin[1], B. Keimer[1] and V. Hinkov[1]*

Magnetic Cooper-pairing mechanisms have been proposed for heavy-fermion and cuprate superconductors; however, strong electron correlations[1] and complications arising from a pseudogap[2–4] or competing phases[5] have precluded commonly accepted theories. In the iron arsenides, the proximity of superconductivity and antiferromagnetism in the phase diagram[6,7], the apparently weak electron–phonon coupling[8] and the 'resonance peak' in the superconducting spin-excitation spectrum[9–11] have also fostered the hypothesis of magnetically mediated Cooper pairing. However, as most theories of superconductivity are based on a pairing boson of sufficient spectral weight in the normal state, detailed knowledge of the spin-excitation spectrum above the superconducting transition temperature T_c is required to assess the viability of this hypothesis[12,13]. Using inelastic neutron scattering we have studied the spin excitations in optimally doped $BaFe_{1.85}Co_{0.15}As_2$ ($T_c = 25$ K) over a wide range of temperatures and energies. We present the results in absolute units and find that the normal-state spectrum carries a weight comparable to that in underdoped cuprates[14,15]. In contrast to cuprates, however, the spectrum agrees well with predictions of the theory of nearly antiferromagnetic metals[16], without the aforementioned complications. We also show that the temperature evolution of the resonance energy monotonically follows the closing of the superconducting energy gap Δ, as expected from conventional Fermi-liquid approaches[17,18]. Our observations point to a surprisingly simple theoretical description of the spin dynamics in the iron arsenides and provide a solid foundation for models of magnetically mediated superconductivity.

In conventional superconductors such as mercury or niobium, the electron system gains energy by establishing a superconducting condensate consisting of Cooper pairs bound by the exchange of virtual phonons. Other elementary excitations also have the potential to mediate pairing: in heavy-fermion superconductors such as $CeCoIn_5$ or UPd_2Al_3, antiferromagnetic (AFM) spin excitations are likely to be involved in the pairing mechanism[1]. However, coupling of itinerant carriers to the quasi-localized rare-earth f-electrons introduces a complexity that has hitherto precluded a commonly accepted theory[1].

In cuprate high-T_c superconductors, AFM spin excitations are also among the most promising contenders for the pairing boson[19], despite the remaining controversy about the role of electron–phonon interactions. Here, the complication comes from strong electron interactions in the form of on-site Coulomb repulsion, which render the parent compounds AFM Mott insulators, and from a multitude of poorly understood phenomena, such as the normal-state pseudogap and the competition of superconductivity with incommensurate spin- and charge-modulated phases[5]. Even the adequacy of boson-mediated pairing schemes itself has been called into question[20].

The recently discovered iron arsenide superconductors are characterized by AFM correlations throughout the phase diagram, often coexisting with superconductivity deep into the superconducting dome[7]. Besides, it was shown[8] that electron–phonon coupling is too weak to explain the high T_c, which turns the spotlight onto the magnetic coupling channel again[21,22]. Although iron arsenides also derive from AFM parents, unlike cuprates they remain metallic at all doping levels, rendering Fermi-liquid-based approaches more promising than for cuprates.

In several of these unconventional superconductors, a redistribution of AFM spectral weight into a 'resonance peak' at an energy $\hbar\omega = \hbar\omega_{res}$ smaller than the superconducting gap 2Δ heralds the onset of superconductivity[1,3,23]. As the intensity of this mode is determined by coherence factors in the superconducting gap equation, it is only expected to occur for particular gap symmetries and was one of the first indications for d-wave superconductivity in the cuprates. The recent discovery of a resonant mode in both hole-doped $Ba_{1-x}K_xFe_2As_2$ (ref. 9) and electron-doped $BaFe_{2-x}(Ni,Co)_xAs_2$ (refs 10, 11) is therefore an important achievement. Although the existence of a resonance was shown to be compatible with a sign-reversed $s_{\pm}$-wave superconducting gap[17,18], it is a consequence of the opening of the gap and hence does not *per se* constitute evidence of a magnetic pairing mechanism. As a pairing boson of sufficient spectral weight must be present already above T_c, detailed knowledge of both the spectrum in the normal state and its redistribution below T_c is a prerequisite for a quantitative assessment of theoretical models, as recently demonstrated for $YBa_2Cu_3O_{6.6}$ (ref. 13).

Here we study the spin excitations in a single crystal of optimally electron-doped $BaFe_{1.85}Co_{0.15}As_2$ ($T_c = 25$ K) at temperatures up to $T = 280$ K and energies up to $\hbar\omega = 32$ meV ($>4\Delta$). We begin by showing in Fig. 1a the scattering function $S(\mathbf{Q},\omega)$ at the AFM wavevector $\mathbf{Q} = \mathbf{Q}_{AFM} = ((1/2)\,(1/2)\,1)$ for $\hbar\omega \leq 15$ meV in the superconducting state (4 K) and in the normal state (60 K). The

[1]Max-Planck-Institut für Festkörperforschung, Heisenbergstraße 1, 70569 Stuttgart, Germany, [2]Laboratoire Léon Brillouin, CEA-CNRS, CEA Saclay, 91191 Gif-sur-Yvette Cedex, France, [3]Institut für Festkörperphysik, Technische Universität Dresden, D-01062 Dresden, Germany, [4]Forschungsneutronenquelle Heinz Maier-Leibnitz (FRM-II), TU München, D-85747 Garching, Germany, [5]Institut für Physikalische Chemie, Universität Göttingen, 37077 Göttingen, Germany. *e-mail: V.Hinkov@fkf.mpg.de.

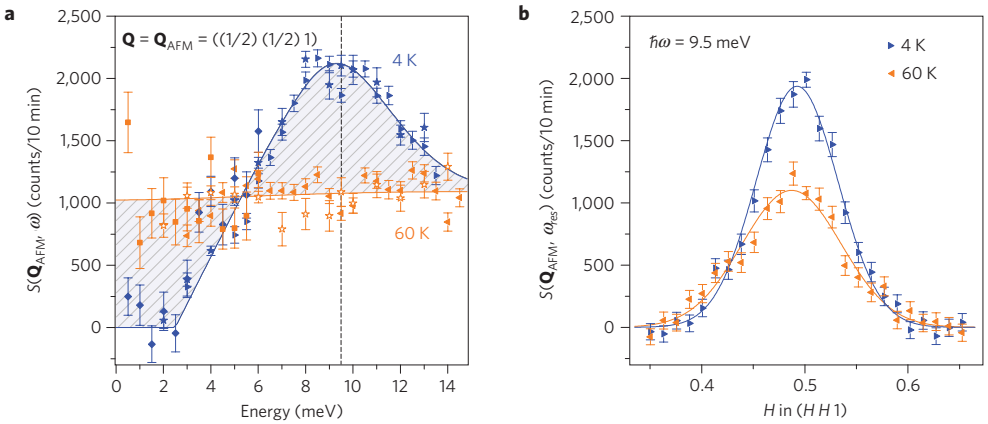

Figure 1 | Spin excitations in the vicinity of the AFM wavevector $\mathbf{Q}_{\mathbf{AFM}}$, in the superconducting ($T = 4$ K) and the normal state ($T = 60$ K). a, Energy evolution of the magnetic scattering function $S(\mathbf{Q}_{\mathrm{AFM}}, \omega)$ after a background correction. The different symbol shapes represent measurements at different spectrometers (see the Methods section). The solid lines are guides to the eye. **b**, Wavevector dependence of $S(\mathbf{Q}, \omega)$ measured at the resonance energy (dashed line in **a**). A linear background has been subtracted. The lines are Gaussian fits. The error bars represent the statistical error.

data were obtained by collecting a series of $\mathbf{Q}$-scans at fixed ω, and ω-scans at fixed $\mathbf{Q}_{\mathrm{AFM}}$, supplemented by points appropriately offset from $\mathbf{Q}_{\mathrm{AFM}}$ to allow an accurate background subtraction. We determine $\hbar\omega_{\mathrm{res}}$ to be 9.5 meV, in agreement with previous investigations on samples of similar doping levels[11]. At this stage, we present $S(\mathbf{Q}, \omega)$ instead of the dynamical susceptibility $\chi''(\mathbf{Q}, \omega)$, because a sum rule holds, stipulating that $\int_{-\infty}^{\infty} \mathrm{d}\omega \int \mathrm{d}\mathbf{Q}\, S(\mathbf{Q}, \omega)$ is T-independent. An important result is that within the experimental error the resonant spectral-weight gain is compensated by a depletion at low energies, and that the superconductivity induced effects are limited to $\hbar\omega \lesssim 2\Delta$ (see also Fig. 2). The $\mathbf{Q}$-integration can be neglected here, because within the shown energy range of up to 2Δ the spectrum remains commensurate and the measured $\mathbf{Q}$-width does not change appreciably (Fig. 1b and Supplementary Information). Its value of ~0.1 r.l.u. is much broader than the resolution and thus represents the intrinsic $\mathbf{Q}$-width to a good approximation. Furthermore, the energy width of the resonance of ~6 meV is not resolution limited.

We next obtain $\chi''(\mathbf{Q}_{\mathrm{AFM}}, \omega)$ by correcting $S(\mathbf{Q}_{\mathrm{AFM}}, \omega)$ for the thermal population factor, which is largest at low ω and high T (Fig. 2). Carrying out this correction, we now clearly establish that the low-ω suppression represents a full depletion and not a trivial thermal-population effect. One of the central results of our study is that we can present $\chi''(\mathbf{Q}, \omega)$ in absolute units (see the Methods section). Apart from its importance for theoretical work, this allows us to extract the weight of the spectral features to be discussed below.

In the normal state at 60 K we observe a broad spectrum of gapless excitations with a maximum around 20 meV and a linear ω-dependence for $\omega \to 0$. Increasing T to 280 K suppresses the intensity and presumably shifts the maximum to higher energies, while the low-energy linearity is preserved. This behaviour and the absence of complications by incommensurate modulations or a pseudogap (see also Fig. 3a) motivates an analysis within the framework of the theory of nearly AFM Fermi liquids[16], for which

$$\chi''_T(\mathbf{Q}, \omega) = \frac{\chi_T \Gamma_T \omega}{\omega^2 + \Gamma_T^2 \left(1 + \xi_T^2 |\mathbf{Q} - \mathbf{Q}_{\mathrm{AFM}}|^2\right)^2}$$

Here $\chi_T = \chi_0 (T + \Theta)^{-1}$ represents the strength of the AFM correlations in the normal state, $\Gamma_T = \Gamma_0 (T + \Theta)$ is the damping constant, $\xi_T = \xi_0 (T + \Theta)^{-1/2}$ is the magnetic correlation length and Θ is the Curie–Weiss temperature. We obtain the best fit to all of the normal-state data for

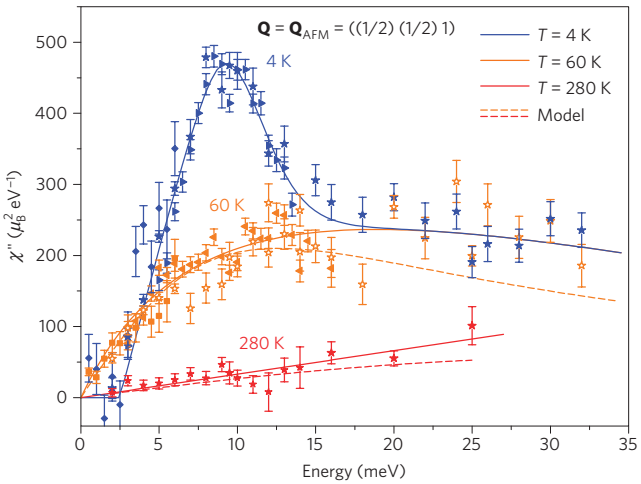

Figure 2 | Imaginary part of the spin susceptibility $\chi(\mathbf{Q}_{\mathbf{AFM}}, \omega)$ in the superconducting ($T = 4$ K) and the normal state ($T = 60$ and 280 K). The data were obtained from $S(\mathbf{Q}, \omega)$ by correcting for the thermal-population factor and were put on an absolute scale as described in the Supplementary Information. The solid lines are guides to the eye. The dashed lines represent global fits of the formula described in the text to all of the normal-state data in this figure and Figs 1 and 3. The different symbol shapes are consistent with Fig. 1 and represent measurements at different spectrometers (see the Methods section). The error bars represent the statistical error.

$\chi_0 = (3.8 \pm 1.0) \times 10^4\, \mu_{\mathrm{B}}^2\, \mathrm{K\,eV^{-1}}$, $\Gamma_0 = (0.14 \pm 0.04)\, \mathrm{meV\,K^{-1}}$, $\Theta = (30 \pm 10)$ K and $\xi_0 = (163 \pm 20)\, \mathrm{\AA\,K^{1/2}}$, shown as dashed lines in Fig. 2. The deviation of the model from the experimental data at high energies can possibly be explained by the presence of several bands in the system, which shifts the maximum of $\chi''_{60\,\mathrm{K}}(\mathbf{Q}_{\mathrm{AFM}}, \omega)$ to a higher value of ~20 meV. The total spectral weight at 60 K, integrated over $\mathbf{Q}$ and ω up to 35 meV, is $\chi''_{60\,\mathrm{K}} = 0.17\, \mu_{\mathrm{B}}^2$/f.u., and is thus comparable to underdoped $YBa_2Cu_3O_{6+x}$ (ref. 14). The net resonance intensity, on the other hand, amounts to $\chi''_{\mathrm{res}} = \chi''_{4\,\mathrm{K}} - \chi''_{60\,\mathrm{K}} = 0.013\, \mu_{\mathrm{B}}^2$/f.u., which is 3–5 times smaller than in $YBa_2Cu_3O_{6+x}$ (ref. 14).

From Fig. 2 we can define three energy intervals: the spin gap below ~3 meV, the resonance region between ~3 and ~15 meV and the region above ~15 meV with no superconductivity-induced changes. Figure 3a shows the evolution of $\chi''(\mathbf{Q}_{\mathrm{AFM}}, \omega)$ at the representative energies 3, 9.5 and 16 meV for temperatures up to

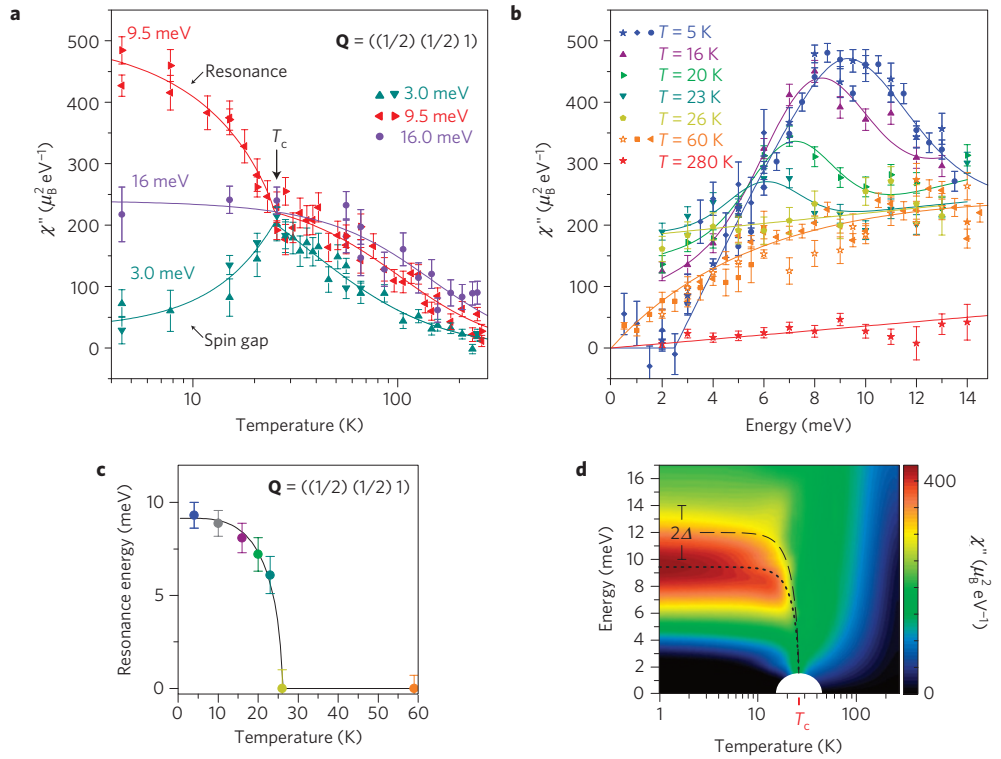

Figure 3 | Energy and temperature dependence of $\chi''(\mathbf{Q}_{AFM},\omega)$ and evolution of the resonance peak below T_c. a, Temperature dependence of $\chi''(\mathbf{Q}_{AFM},\omega)$ at three different energies: within the spin gap (3 meV), at $\hbar\omega_{res}$ (9.5 meV) and above 2Δ (16 meV). **b**, Energy scans at $\mathbf{Q}_{AFM}$ showing $\chi''(\mathbf{Q},\omega)$ at different temperatures. The lines in **a** and **b** are guides to the eye; the error bars represent the statistical error. **c**, Temperature evolution of the resonance energy $\hbar\omega_{res}(T)$ defined by the maxima in **b**. The line has the same functional dependence as the superconducting gap Δ obtained by angle-resolved photoemission[24,25], that is $\omega_{res}(T) \propto \Delta(T)$. **d**, Interpolation of the data in **a** and **b** showing $\chi''(\mathbf{Q}_{AFM},\omega)$ in the ω–T plane for T up to 280 K. The vertical bar shows the interval of the reported 2Δ values[25–27]. The dotted line is the same as the fit in **c**. The dashed line has the same functional dependence and tracks the average value of $2\Delta(T)$ as a function of T. Note the logarithmic T-scale in **a** and **d**.

280 K. We observe a smooth increase on cooling down to T_c at all three energies. Whereas at 16 meV the intensity also evolves smoothly across T_c, there are pronounced anomalies at 3 and 9.5 meV, indicating the abrupt gap opening. We note that there is no indication of a pseudogap opening above T_c, which is consistent with the linear behaviour of $\chi''(\mathbf{Q},\omega)$ at small ω (Fig. 2).

However, because the superconducting gap decreases on heating to T_c (refs 24, 25), it does not suffice to study the T-dependence of $\chi''(\mathbf{Q},\omega)$ at a fixed energy. Hence, we investigated the evolution of the resonance peak by carrying out energy scans at several temperatures below T_c (Fig. 3b). An important result is that $\hbar\omega_{res}$ decreases on heating as well, and it follows the same functional dependence as Δ with remarkable precision, that is $\hbar\omega_{res}(T) \propto \Delta(T)$ (Fig. 3c).

A comprehensive summary of our data in the ω–T plane is shown in Fig. 3d. An extended animation thereof, including the $\mathbf{Q}$-dependence, is presented in the Supplementary Information. As indicated by the vertical bar, the resonance maximum always remains inside the 2Δ gap, although its tail might extend beyond. The value of $\Delta = (6 \pm 1)$ meV that we use for the superconducting gap is an average of the reported experimental values obtained by a number of different methods[25–27].

What are the implications of our results for the physics and in particular the superconducting mechanism of the iron arsenides? We begin by comparing the normal-state spin excitations of $BaFe_{1.85}Co_{0.15}As_2$ to those of the cuprates. Remarkably, the overall magnitude of $\chi''(\mathbf{Q},\omega)$ is similar in both families[14,15]. However, the cuprate spectra show anomalous features such as a 'spin pseudogap'[3,4] and a broad peak reminiscent of the resonant mode in the normal state[14]. In contrast, we have shown that the normal-state spin-excitation spectrum of $BaFe_{1.85}Co_{0.15}As_2$ is gapless and can be well described by a simple formula for nearly AFM metals[16]. We point out that despite the comparable normal-state magnitude of $\chi''(\mathbf{Q},\omega)$ in iron arsenides and cuprates, T_c and the resonance enhancement of $\chi''(\mathbf{Q},\omega)$ below T_c are significantly lower in the former, which is an indication that the spin–fermion coupling is weaker in arsenides than in cuprates.

Turning now to the superconducting state, we first note that the impact of superconductivity on the spin excitations can be fully accounted for by the opening of Δ and the appearance of the resonance, without qualitative changes to the excitation geometry. Considering the resonance as a bound state within the superconducting gap, $\hbar\omega_{res} < 2\Delta$ is required, and our value of $\hbar\omega_{res}/2\Delta = (0.79 \pm 0.15)$ is in good agreement with the predictions for a sign-reversed $s_{\pm}$-wave gap[17,18]. Furthermore, we have shown that $\hbar\omega_{res}$ monotonically decreases with the closing of the gap $\Delta(T)$ on heating, as expected from conventional Fermi-liquid-based approaches[28]. Once more, the simplicity of this behaviour is in notable contrast to its counterpart in the cuprates[23], where the temperature insensitivity of $\hbar\omega_{res}$ has inspired theories that attribute the spin resonance to a collective mode characteristic of a state competing with superconductivity[29]. However, we also point out that the value we obtain for $\hbar\omega_{res}/2\Delta$ is larger but not very far from the value of 0.64 reported in ref. 30 to constitute a universal value connecting the resonance phenomena in cuprates, heavy-fermion superconductors and arsenides. Clearly, more precise measurements of Δ are necessary.

Finally, although in contrast to hole-hoped $Ba_{1-x}K_xFe_2As_2$ (ref. 24) conclusive evidence for two distinctly different superconducting gaps in $BaFe_{2-x}Co_xAs_2$ has not yet been presented, the

multiband character should be kept in mind when discussing the iron arsenides—this can, for instance, contribute to the observed width of the resonance. We also mention that for the moment the observed pinning of spin excitations to $\mathbf{Q}_{\mathrm{AFM}}$ cannot be reconciled with predictions of incommensurate excitations[18] based on the notion that the nesting vector should deviate from $\mathbf{Q}_{\mathrm{AFM}}$ owing to electron-doping-related Fermi-surface changes.

The comprehensive set of data on the spin dynamics in $BaFe_{1.85}Co_{0.15}As_2$ in the normal and superconducting states we have presented will allow a rigorous assessment of spin-fluctuation-mediated pairing models for the iron arsenides. In particular, on the basis of our absolute-unit calibration of $\chi''(\mathbf{Q},\omega)$ it will become possible to compare the total exchange energy of the electron system below T_c to the condensation energy determined by specific-heat measurements[31]. Independent information about the spin–fermion coupling strength can also be derived from a comparison of the measured spin fluctuation spectrum and the fermionic self-energy extracted from photoemission spectroscopy. Although these complementary approaches have yielded important insights into the mechanism of superconductivity in cuprates[13,32], a controlled, commonly accepted theory is still missing. Our data provide tantalizing indications that such a theory may be obtainable for the iron arsenides.

Methods

Our sample is a single crystal of $BaFe_{1.85}Co_{0.15}As_2$ with a mass of 1.0 g. It was grown with the self-flux method to prevent contaminations, and using a nucleation centre. The high crystalline quality was assessed by neutron- and X-ray diffraction measurements. The superconducting transition temperature was determined by superconducting quantum interference device magnetometry to be $T_c = 25$ K, which corresponds to an optimal doping level according to the phase diagram[6].

We use tetragonal notation and quote the transferred wavevector $\mathbf{Q}$ in units of the reciprocal lattice vectors a^*, b^* and c^*. In this notation, the AFM wavevector is $\mathbf{Q}_{\mathrm{AFM}} = ((1/2)\,(1/2)\,1)$.

The data were collected using the cold triple-axis Panda and thermal triple-axis Puma spectrometers (FRM-II, Garching, Germany), as well as the 2 T spectrometer (LLB, Saclay, France). In Figs 1 and 2, the corresponding data sets are marked with squares, triangles and stars, respectively. The sample was mounted into a standard cryostat with the (110) and (001) directions in the scattering plane. In all cases, pyrolytic graphite monochromators and analysers were used. Measurements were carried out in constant-k_f mode, with $k_f = 1.55$ Å^{-1} in conjunction with a beryllium filter at small ω and $k_f = 2.66$ Å^{-1} or $k_f = 4.1$ Å^{-1} with a pyrolytic graphite filter at large ω. Wherever applicable, the background was subtracted from the data, and corrections for the magnetic structure factor and for the energy-dependent fraction of higher-order neutrons were applied. The imaginary part of the dynamical spin susceptibility $\chi''(\mathbf{Q},\omega)$ was obtained from the scattering function $S(\mathbf{Q},\omega)$ by the fluctuation–dissipation relation $\chi''(\mathbf{Q},\omega) = (1 - \mathrm{e}^{-\hbar\omega/k_B T})\, S(\mathbf{Q},\omega)$. The data sets measured at different spectrometers or with different experimental settings were scaled by using overlapping energy regions as a reference. The error bars in all figures correspond to one standard deviation of the count rate and do not include the normalization errors.

We put our data on an absolute scale by comparing the magnetic scattering intensity to the intensity of acoustic phonons as well as nuclear Bragg peaks after taking care of resolution corrections. This approach is extensively discussed in ref. 14 and references therein, from which we also adopt the definition of χ'' as $\mathrm{Tr}\,\chi''_{\alpha\beta}/3$, where $\chi''_{\alpha\beta}$ is the imaginary part of the generalized susceptibility tensor.

Received 29 June 2009; accepted 23 November 2009; published online 20 December 2009

References

1. Sato, N. K. *et al.* Strong coupling between local moments and superconducting 'heavy' electrons in UPd_2Al_3. *Nature* **410,** 340–343 (2001).
2. Norman, M. R., Pines, D. & Kallin, C. The pseudogap: Friend or foe of high T_c? *Adv. Phys.* **54,** 715–733 (2005).
3. Rossat-Mignod, J. *et al.* Neutron scattering study of the $YBa_2Cu_3O_{6+x}$ system. *Physica C* **185,** 86–92 (1991).
4. Lee, C. H., Yamada, K., Hiraka, H., Venkateswara Rao, C. R. & Endoh, Y. Spin pseudogap in $La_{2-x}Sr_xCuO_4$ studied by neutron scattering. *Phys. Rev. B* **67,** 134521 (2003).
5. Tranquada, J. M., Sternlieb, B. J., Axe, J. D., Nakamura, Y. & Uchida, S. Evidence for stripe correlations of spins and holes in copper oxide superconductors. *Nature* **375,** 561–563 (1995).
6. Chu, J.-H., Analytis, J. G., Kucharczyk, C. & Fisher, I. R. Determination of the phase diagram of the electron-doped superconductor $Ba(Fe_{1-x}Co_x)_2As_2$. *Phys. Rev. B* **79,** 014506 (2009).
7. Drew, A. J. *et al.* Coexistence of static magnetism and superconductivity in $SmFeAsO_{1-x}F_x$ as revealed by muon spin rotation. *Nature Mater.* **8,** 310–314 (2009).
8. Boeri, L., Dolgov, O. V. & Golubov, A. A. Is $LaFeAsO_{1-x}F_x$ an electron–phonon superconductor? *Phys. Rev. Lett.* **101,** 026403 (2008).
9. Christianson, A. D. *et al.* Unconventional superconductivity in $Ba_{0.6}K_{0.4}Fe_2As_2$ from inelastic neutron scattering. *Nature* **456,** 930–932 (2008).
10. Li, S. *et al.* Spin gap and magnetic resonance in superconducting $BaFe_{1.9}Ni_{0.1}As_2$. *Phys. Rev. B* **79,** 174527 (2009).
11. Lumsden, M. D. *et al.* Two-dimensional resonant magnetic excitation in $BaFe_{1.84}Co_{0.16}As_2$. *Phys. Rev. Lett.* **102,** 107005 (2009).
12. Parks, R. D. (ed.) *Superconductivity* Vol. 1 (Dekker, 1969).
13. Dahm, T. *et al.* Strength of the spin-fluctuation-mediated pairing interaction in a high-temperature superconductor. *Nature Phys.* **5,** 217–221 (2009).
14. Fong, H. F. *et al.* Spin susceptibility in underdoped $YBa_2Cu_3O_{6+x}$. *Phys. Rev. B* **61,** 14773–14786 (2000).
15. Lipscombe, O. J., Vignolle, B., Perring, T. G., Frost, C. D. & Hayden, S. M. Emergence of coherent magnetic excitations in the high temperature underdoped $La_{2-x}Sr_xCuO_4$ superconductor at low temperatures. *Phys. Rev. Lett.* **102,** 167002 (2009).
16. Moriya, T. *Spin Fluctuations in Itinerant Electron Magnetism* (Springer, 1985).
17. Korshunov, M. M. & Eremin, I. Theory of magnetic excitations in iron-based layered superconductors. *Phys. Rev. B* **78,** 140509 (2008).
18. Maier, T. A., Graser, S., Scalapino, D. J. & Hirschfeld, P. Neutron scattering resonance and the Fe-pnictide superconducting gap. *Phys. Rev. B* **79,** 134520 (2009).
19. Eschrig, M. The effect of collective spin-1 excitations on electronic spectra in high-T_c superconductors. *Adv. Phys.* **55,** 47–183 (2006).
20. Anderson, P. W. Is there a glue in cuprate superconductors. *Science* **316,** 1705–1707 (2007).
21. Mazin, I. I., Singh, D. J., Johannes, M. D. & Du, M. H. Unconventional superconductivity with a sign reversal in the order parameter of $LaFeAsO_{1-x}F_x$. *Phys. Rev. Lett.* **101,** 057003 (2008).
22. Graser, S., Maier, T. A., Hirschfeld, P. J. & Scalapino, D. J. Near-degeneracy of several pairing channels in multiorbital models for the Fe pnictides. *New J. Phys.* **11,** 025016 (2009).
23. Fong, H. F., Keimer, B., Reznik, D., Milius, D. L. & Aksay, I. A. Polarized and unpolarized neutron-scattering study of the dynamical spin susceptibility of $YBa_2Cu_3O_7$. *Phys. Rev. B* **54,** 6708–6720 (1996).
24. Evtushinsky, D. V. *et al.* Momentum dependence of the superconducting gap in $Ba_{1-x}K_xFe_2As_2$. *Phys. Rev. B* **79,** 054517 (2009).
25. Terashima, K. *et al.* Fermi surface nesting induced strong pairing in iron-based superconductors. *Proc. Natl Acad. Sci. USA* **106,** 7330–7333 (2009).
26. Samuely, P. *et al.* Point contact Andreev reflection spectroscopy of superconducting energy gaps in 122-type family of iron pnictides. *Physica C* **469,** 507–511 (2009).
27. Yin, Y. *et al.* Scanning tunnelling spectroscopy and vortex imaging in the iron pnictide superconductor $BaFe_{1.8}Co_{0.2}As_2$. *Phys. Rev. Lett.* **102,** 097002 (2009).
28. Abanov, A. & Chubukov, A. V. A relation between the resonance neutron peak and ARPES data in cuprates. *Phys. Rev. Lett.* **83,** 1652–1655 (1999).
29. Morr, D. K. & Pines, D. The resonance peak in cuprate superconductors. *Phys. Rev. Lett.* **81,** 1086–1089 (1998).
30. Yu, G., Li, Y., Motoyama, E. M. & Greven, M. A universal relationship between magnetic resonance and superconducting gap in unconventional superconductors. *Nature Phys.* **5,** 873–875 (2009).
31. Demler, E. & Zhang, S. Quantitative test of a microscopic mechanism of high-temperature superconductivity. *Nature* **396,** 733–735 (1998).
32. Woo, H. *et al.* Magnetic energy change available to superconducting condensation in optimally doped $YBa_2Cu_3O_{6.95}$. *Nature Phys.* **2,** 600–604 (2006).

Acknowledgements

The project was supported, in part, by the DFG in the consortium FOR538. We are grateful to L. Boeri, T. Dahm, O. Dolgov, D. Efremov, I. Eremin, D. Evtushinsky, G. Jackeli, G. Khaliullin, A. Yaresko and R. Zeyher for stimulating discussions and numerous helpful suggestions.

Author contributions

D.L.S. and C.T.L. synthesized the sample. D.S.I., J.T.P., P.B., Y.S., A.S., K.H. and D.H. carried out the measurements. D.S.I., J.T.P., P.B. and V.H. analysed the data. D.S.I., V.H. and B.K. wrote the manuscript. V.H. and B.K. planned and managed the project.

Additional information

The authors declare no competing financial interests. Supplementary information accompanies this paper on www.nature.com/naturephysics. Reprints and permissions information is available online at http://npg.nature.com/reprintsandpermissions. Correspondence and requests for materials should be addressed to V.H.